Topological Optimization of an Interface Metal Structure

Rafael Vieira De Sequeira
rafael.vieira.de.sequeira@tecnico.ulisboa.pt

Instituto Superior Técnico, Universidade de Lisboa, Portugal

October 2018

Abstract

In this paper, a metal interface structure with high mechanical requirements for vibrating tests is developed. This work starts by portraying the several advantages of Topological Optimization and Additive Manufacturing in components with high requirements in the aerospacial sector with the purpose of use these technologies combination to improve *Active Space Technologies* current interface structure for vibration experimental tests.

In order to expand the author's knowledge in the Topological Optimization field, several benchmark examples were analysed and compared with literature's known results. Using this base knowledge, the optimization process methodology was developed and implemented with success. This methodology was validated through an experimental vibration activity that was compared with the numerical model's results. This process was developed with different requirements from the metal structure's ones since the used material is a polymer.

The final metal structure optimization and design process is based on the validated methodology and presents significant improvements when compared to the company's current solution.

Keywords: Additive Manufacturing, Mass Reduction , Modal Analysis, Optistruct, Topological Optimization

1. Introduction

The aerospace industry is looking for new developments and some of the most important concerns are the structure's weight in order to save on fuel consumption while improving the structural efficiency of the structures. Both these goals can be achieved by combining a Topology Optimization (TO) technique with an Additive Manufacture (AM) process.

TO intends to find an optimal structural configuration within a given design domain for specified objectives, constraints, boundary conditions and loads where its biggest advantage over sizing or shape optimizations lies in the fact that no specified initial structural topology needs to be presumed. Due to this key advantage, TO had remarkable developments over the last decades in both theoretical studies and practical applications in several industries, [3, 9]. The most popular and successful method in TO due to its simplicity in both conception and numerical implementation was proposed by Bendsøe and is known as Solid Isotropic Material with Penalty (SIMP) [10].

The aerospace industry already shown that significant weight savings can be achieved if TO is used at its fullest. However, it is hard to reproduce such a complex geometry as shown in figure 1 or even worse geometries with subtractive methods. The recent developments in AM enables the potential of TO to be further used, turning this in a perfect combination. This will allow the production of very complex structures without wasting material and without increasing the number of necessary steps until the final product which usually is very time consuming and expensive.

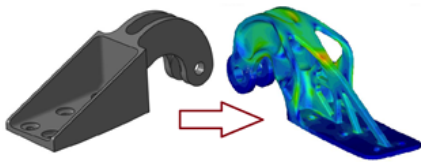

Figure 1: Original and topological optimized A320 hinge bracket, adapted from [13].

A successful example of these technologies combination in the aerospace industry is the weight's saving achieved in the nacelle hinge bracket from an Airbus A320. By optimizing the part, it was possible to reduce the mass from 918g to 326g which represent a 64% mass reduction. The optimized design retained the same characteristics in terms of stiffness and bolt loading, while reducing the stresses on the part. Figure 1 shows the part before and after optimization [13].

1.1. Problem overview and objectives

Active Space Technologies uses an interface structure (L-Shape structure - figure 2) between their Vibration Test System (Shaker) and the hardware part that needs to be tested. The interface structure needs to be as light as possible while ensuring structural intigrity and a minimum of 2500Hz for the first frequency mode. The challenge is to produce a lighter structure than their current solution through the advantages that comes from the combination of TO with AM.

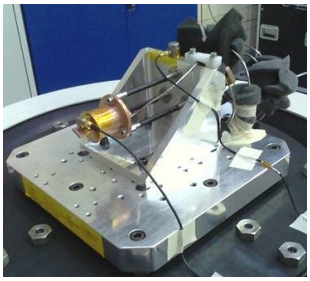

Figure 2: *Active Space Technologies* current solution.

2. Technical Background

2.1. Finite Element Method

The Finite Element Method (FEM) is a numerical method that discretize a continuous geometry (domain) in a mesh of elements (subdomain) with a finite size. The reason to discretize a continuous geometry is to seek an approximate solution on the collection of the subdomains which is easier to solve numerically. This method allows the study of very complex structures and it is a powerful tool in real world application problems. To better understand the method, reference [6] must be seen.

There are 6 different elements present in this work that will only be enumerated. To better understand each element characteristics, Altair Engineering [2] and MSC Software [8] must be consulted.

- 1D elements - rigid RBE2, CBAR and mass element CONM2;
- 2D elements - CQUAD4 with PSHELL properties;
- 3D elements - Brick and Tetrahedral (Tetra) elements with PSOLID properties.

2.1.1 Modal analysis

From Lagrange's equation with a harmonic response assumption, an eigenvalues problem can be develope to find the undamped natural frequencies of a structure in free vibration. The eigenvalues correspond to the natural frequencies (ω_i) and the eigenvectors to the corresponding mode shapes ($\{\Phi\}^i$) obtained by solving the following eigenvalue/eigenvector problem (equation 1).

$$([K] - \omega_i^2[M])\{\Phi\}^i = \{0\} \tag{1}$$

2.1.2 Linear static analysis

One of the simplest analysis with FEM is the linear static analysis which is characterized by considering time independency (static conditions) and only small displacements. Thus, a linear relation is used between the applied load and the system response. A linear static problem is solved through equation 2 where $[K]$ is the stiffness matrix, $\{u\}$ is the nodal displacement vector and $\{F\}$ is the nodal forces vector.

$$[K]\{u\} = \{F\} \tag{2}$$

2.1.3 Failure criterion

An accurate failure criterion is essential to correctly design any mechanical component. In applications where isotropic and ductile materials are used, it is common to use a yield criterion such as Von Mises. However, since the company follows ECSS-E-ST-32C Rev. 1 standard from the European Cooperation for Space Standardization (ECSS), this criterion must be used together with a Margin of Safety (MoS) which can be calculated through equation 3, where $\sigma_{allowable}$ is the defined allowable stress limit, $\sigma_{applied}$ is the present stress and the FoS is the Factor of Safety defined as 2 for the elastic regime. Besides, this structure will be used in high frequency load conditions which can lead to fatigue failures that should be also taken into account.

$$MoS = \frac{\sigma_{allowable}}{\sigma_{applied} \cdot FoS} - 1 \tag{3}$$

2.2. Topological Optimization

The SIMP method is based on an equivalent element Young's modulus (E_e) as function of the relative element density (x_e) and the solid material Young's modulus (E_0). This function is given by equation 4.

$$E_e(x_e) = x_e^p E_0, \quad 0 < x_{min} \leq x_e \leq 1 \tag{4}$$

where p is a penalization power that should be higher than 1, usually 3 ($1< p <7$). x_{min} is the relative element density of the void material, which is higher than zero to avoid singularity of the finite element stiffness matrix, that occurs if all material is removed. So, a hole is represented by elements with density of x_{min} or near.

A modified SIMP approach given by equation 5 can be used where Young's modulus of the void or weak material is defined as E_{min}. This is a non-zero value to avoid singularity of the finite element stiffness matrix as explained before.

$$E_e(x_e) = E_{min} + x_e^p(E_0 - E_{min}), \quad x_e \in [0, 1] \tag{5}$$

Using the finite element analysis theory, the global stiffness matrix (K) is defined by equation 6a and the element stiffness matrix (K_e) defined by equation 6b.

$$K(x) = \sum_{e=1}^{N} K_e(x_e) \tag{6a}$$

$$K_e(x_e) = E_e(x_e)k_e^0 \tag{6b}$$

where k_e^0 is the element stiffness matrix for an element with an unitary Young's modulus, which implies that this matrix is independent of the elastic modulus, and therefore independent of x_e. The k_e^0 matrix depends on the element type and the Poisson's ratio (ν).

3. Methodology

3.1. Benchmark problems

Two classical topology optimization problems - 2D Messerschmidt-Blkow-Blohm (MBB) beam and 3D Cantilevered beam were used to improve the author's knowledge in this field. The problems were modelled using CQUAD4 and Brick elements and the objective was to gain sensitivity to the several TO parameters influence during the optimization process. This was achieved through the comparison of the used commercial softwares (Altair Optistruct - student version 13.0 and MSC Nastran SOL200 - student version 2017.1) with the already known Matlab's codes [7, 11]. Both benchmark problems use as objective function the minimization of compliance with a constraint in the volume fraction.

In order to study the three biggest variables of interest in TO, 3 models variations for each variable were developed. The results of all these analysis for each variable of interest change are depicted in table 1 and it was possible to conclude that Optistruct presents better results in terms of number of iterations and in the compliance value when compared to Matlab and SOL200.

Most important conclusions for the parameters:

- f has a significant influence over the design geometry and performance (as supposed since it is the optimization constraint);
- The mesh has influence over the geometry complexity and performance but this was not perfectly evaluated due to a "relative refinement" instead of an "absolute refinement" which introduced some "size dependent" problem characteristics;
- p is problem dependent if a ideal value is needed. However, p equal to 3, as recommended by literature, is typically the best choice.

Table 1: Benchmark problems optimization values.

		Matlab		SOL200		Optistruct		
		No. of iterations for convergence	Compliance [Nm]	No. of iterations for convergence	Compliance [Nm]	No. of iterations for convergence	Compliance [Nm]	Parameter
MBB beam - 2D	*f influence*	418	140.06	27	214.61	37	85.78	*f=0.3*
		389	82.28	17	112.78	23	59.23	*f=0.5*
		345	61.67	13	93.43	14	50.32	*f=0.7*
	Mesh influence	94	94.06	30	120.70	31	48.40	*size 1*
		260	85.32	21	108.57	26	53.19	*size 2*
		389	82.28	17	112.78	23	59.23	*size 3*
	p influence	49	69.21	18	114.63	22	58.97	*p=1*
		389	82.28	17	112.78	23	59.23	*p=3*
		222	95.77	19	118.86	24	64.84	*p=6*
Cantilever beam - 3D	*f influence*	487	96.69	46	165.46	33	38.68	*f=0.3*
		341	73.27	30	56.56	26	22.19	*f=0.5*
		162	36.71	25	38.30	18	17.31	*f=0.7*
	Mesh influence	56	42.49	38	49.11	33	15.03	*size 1*
		114	56.28	30	83.19	33	22.67	*size 2*
		341	73.27	30	56.56	26	22.19	*size 3*
	p influence	38	39.86	24	70.31	27	21.60	*p=1*
		341	73.27	30	56.56	26	22.19	*p=3*
		211	59.83	17	83.10	24	22.84	*p=6*

For the software choice, besides the better results, it is important to refer the smoothing tool possibilities in Optistruct for topology results and its Graphical User Interface (GUI) which is easier to use when compared to SOL200, in the author's opinion. So, Optistruct was chosen for the final structure optimization.

3.2. Optimization approach validation

3.2.1 Numerical modelling - general initial model

The structure's initial FEM model is shown on figure 4 and it is characterized by:

- The structure division into two regions:
  - Non-design space (figure 3.2.1a) Essential parts for the structures as the connections points for the screws;
  - Design space (figure 3.2.1b) All the rest of the volume with some assembly constraints. The objective of this design region is to use the outside dimensions of the L-shape structure (company's current solution) at their limit to expand the geometric freedom for the TO. So, a solid rectangular prism with 120mmx120mmx100mm as dimensions is used with some empty spaces to allow the mounting of the hardware system assembly and some of its movement during the experiment. The space for the hardware system is characterized by three holes for the connection tubes and a prism volume cut that allows the hardware system (figure 3.2.1c);

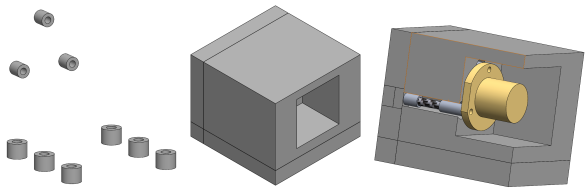

(a) Non-design space. (b) Design space. (c) Hardware system assembly's free space.

Figure 3: General initial model.

- RBE2 elements to simulate the screws in the joints and the connection carbon tubes;
- A CONM2 element instead of a 3D model of the hardware system structure. This element simulates the system's Center of Gravity (CoG);
- Tetra elements with 2mm as global element size for the 3D structure.
- Refined mesh with smooth transitions in the joints to guarantee good accuracy in the critical areas;
- The 6 base's screws joints with the 6 Degrees of Freedom (DoF) fixed.

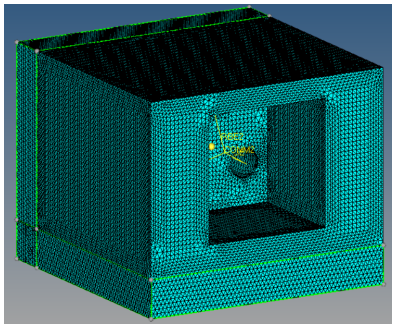

Figure 4: General initial model mesh.

The interface metal structure to be designed has a requirement of a first mode frequency of 2500Hz and 8 load cases with a base inertial acceleration of 60G of magnitude in the 3 principal axis directions with the axis orientation combination as shown on table 2.

Table 2: Load cases orientation - combination matrix.

Load cases			
	x	**y**	**z**
1st load case	+	+	+
2nd load case	+	-	+
3rd load case	+	+	-
4th load case	+	-	-
5th load case	-	+	+
6th load case	-	-	+
7th load case	-	+	-
8th load case	-	-	-

However, for the experimental validation, the available material is the *VisiJet M3 Crystal* polymer [1] that is used on *ProJet MJP 3600* from *3D Systems*. So, proportional load cases were develop for this material where the magnitude of the inertial acceleration was reduced to 1G while the minimum necessary first mode frequency were reduced to 350Hz.

The polymer's mechanical properties were verified through a mechanical characterization activity where ISO 527-1 was used as a guideline since it is a standard for the determination of tensile properties in plastics and is a variant of the standard used by *3D Systems* for the properties in the materials datasheet - ASTM D638. From the obtained results, it was possible to know the material's properties of interest for this work: Young's modulus, yield strength and Poisson's ratio. Besides, it was also possible to know that the material can be assumed as isotropic in the elastic region.

3.2.2 Optimization cycle

The optimization problem formulation used in this work had as objective function the minimization of mass while two constraints should be fulfilled: Minimum first mode frequency as the company demands and maximum stress value below the material's fatigue stress limit with a MoS applied. Still, for the experimental validation, the yield strength was used since the material would not be tested several times and the author didn't characterize the material's fatigue behaviour during the mechanical characterization tests.

The optimization parameters are resumed in table 3 and were based in the author's experience during the benchmark problems phase, material and manufacturing constraints and the company's demands.

Table 3: Optimization model parameters - polymer structure.

E_0	1442.67 MPa
x_{min}	0.001 Kg/m^3
p	3
ν	0.37
Conv.Val	<0.005
Dimension constraint	$\geq$ 0.5 mm
Stress constraint	$\leq$ 10.32 MPa
Frequency constraint	>350 Hz

The final topology was achieved through an optimization cycle composed by 3 phases (figure 5). Every phase had different objectives and relevant findings that are enumerated next:

- **Phase 1:**
  - The design space is the inital one already described with some empty holes for the

screws' heads and washers. The objective is to see the optimal topology for the problem and where the author should remove material to put the Allen wrench during the second phase;

- From the results it was possible to conclude that the stress is not an active constraint since the maximum present value was 7.517e-02MPa. Besides, the general geometry make sense although the two front bolts were probably not necessary.

- **Phase 2:**
  - The design space was reduced to decrease computational cost and the two front bolts were still used but as design space instead of non-design space to confirm if they were really necessary or not. Besides, the space for the Allen wrench was opened;
  - From the obtained results, it was possible to conclude that the two front bolts were not necessary since they didn't have a significant continuity in the material to the rest of the structure. They were only there due to the boundary conditions. The rest of the geometry continues to make sense and it was similar to the previously obtained which was a positive feedback and suggested consistency in the results.

- **Phase 3:**
  - The design space was readapted due to some excessive cuts and the Allen wrench space effect. Besides, the two front bolts were completely removed to achieve a more compact design. In this phase, in order to try a better material distribution, a second design space was created with less material in the center;
  - In general, both designs present similar topologies to the previously obtained which is a positive feedback and suggested consistency in the results. However, by comparing design 3a and 3b topologies, it was possible to conclude that design 3b didn't present any advantage in terms of geometry. Neither by easier assembly mountings nor by better material distribution along the full structure. Instead, design 3b showed significant bigger legs to compensate the lack of material in the middle while 3a presented a compact and continuous material distribution along all linkages.

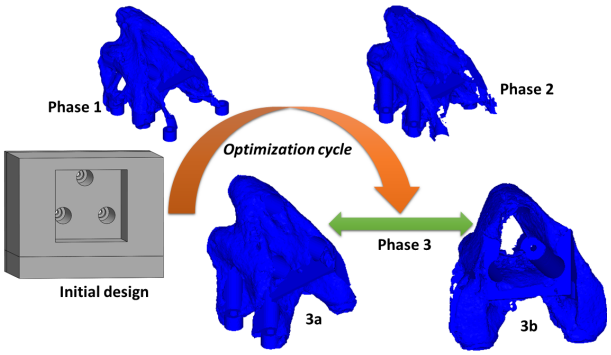

Figure 5: Optimization cycle.

A resume of the optimization cycle characteristics is presented in table 4 and the model mass evolution along the optimization cycle is presented in figure 6.

Based on table 4 and figure 6, it was possible to conclude that the mass of the structure had become smaller during the several phases except for the design 3b, as expected. However, as explained before, this design does not bring any advantage in terms of geometry that could be more valuable than the mass reduction of the structure. So, the final chosen design is the 3a. By analyzing table 4, it was also possible to see that the CPU time significantly increased with the number of elements, as expected. However, the number of iterations didn't appeared to have any relation with the other parameters.

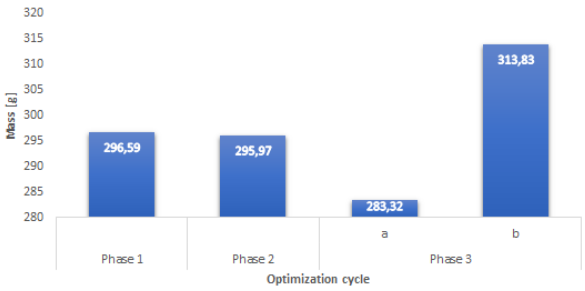

Figure 6: Optimized model mass evolution.

Table 4: Optimization cycle characteristics.

	No. of elements	No. iterations	CPU time [hh:mm:ss]	Frequency [Hz]	Mass [g]
Phase 1	1222022	142	49:00:16	392.63	296.59
Phase 2	635992	182	12:57:43	373.00	295.97
Phase 3 *a*	1009736	348	46:19:52	359.95	283.32
b	955885	276	25:00:46	353.78	313.83

3.2.3 Optimized structure analysis

By using Optistruct's "OSSmooth" tool, it was possible to export the smoothed geometry from the optimization cycle and model it in Solidworks (student version 2016). After the verification of all the relevant assembly issues (figure 7), the structure was

analyzed to confirm if it really fulfilled all the requirements. The connection tubes were modelled as rigid elements since its materials' Young's modulus values are one order of magnitude higher than the interface structure's material.

The analysis results are depicted in table 5 and figure 8. It is possible to see that the 1st mode frequency is 400.92Hz which satisfy the optimization constraint of 350Hz. However, this also proves that the structure could be lighter since this frequency value could be reduced. The only way to have done this was to iterate the CAD modelling with some slight changes and analyze each one of them until the true optimum be achieved. This is not an exact method and therefore, this design was accepted by the author since the main objective of this one was to validate the optimization approach. The present stress value of 0.154MPa was also smaller than the stress constraint of 10.32MPa. Besides, using the same FEM model but without the hardware system, the first mode frequency of the interface structure alone was also calculated with a frequency value of 947.42Hz.

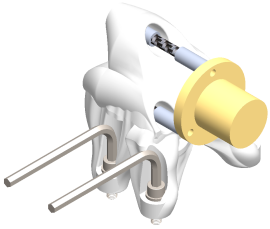

Figure 7: Fully operational assembly.

Table 5: Optimized polymer design - analysis results.

Variables of interest	Results
1st mode frequency [Hz]	400.92
Maximum present stress [MPa]	1.54e-01

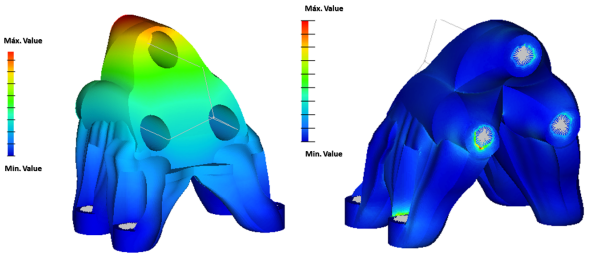

(a) Modal analysis. (b) Static analysis: Stress results.

Figure 8: Optimized polymer design - analysis results.

3.2.4 Optimized structure experimental validation

The experimental activity aims to validate the numerical model and with that, validate the optimization approach used in the designed structure. The interface structure's and assembly's first mode frequency will be assessed through an experimental test in a shaker and if the real frequency value is similar to the theoretical one, the model and the optimization approach are validated.

The test specimen is excited in the *Active Space Technologies* facilities shaker with the input function shown in equation 7 where a is the acceleration, ω is the angular frequency and t is the time. In order to assess the specimen dynamic response and to control the shaker's behaviour, two piezoelectric accelerometers are used: an accelerometer over the specimen (Type 4513-B [4]) and other over the shaker's base (Type 4520-001 [4]). The accelerometer in the shaker's base only measures data in one direction since it is enough to control its translational input. The experimental setup can be seen in figure 9.

$$F(a, \omega, t) = a \cdot \sin(\omega t) \tag{7}$$

(a) Assembly. (b) Interface structure.

Figure 9: Experimental setup.

Software *Shaker Control - version 9.0* is used to monitor, control and acquire the data from the experiment. The obtained results for the assembly and the interface structure alone are shown in figure 10 and 11, respectively. Both graphics have 5 series of data and use a logarithmic scale for the vertical axis. The **Input profile (F)** is the input function which was already explained before as well as its amplitude value (acceleration). The **Control accelerometer** is the data from the accelerometer on the shaker's base. As expected, its values are almost equal to the ones of the **Input profile (F)** and that's why it is not possible to see both in the graphics. The **Accelerometer_X**, **Accelerometer_Y** and **Accelerometer_Z** are the data from the 3 axis of the accelerometer on the specimen.

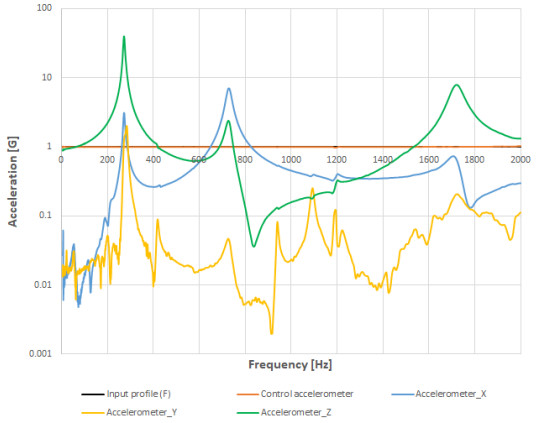

Figure 10: Assembly experimental results.

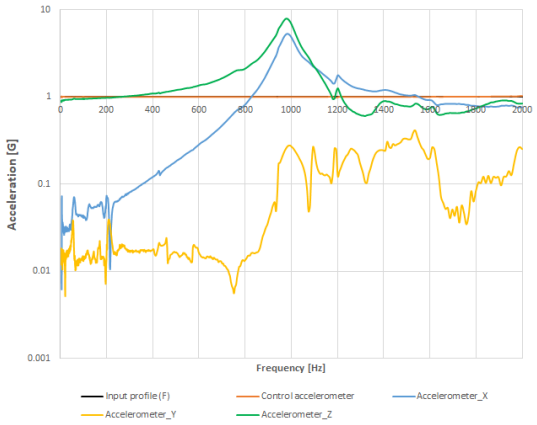

Figure 11: Interface structure experimental results.

The relative difference between the experiment and numerical model results for the assembly and interface structure are depicted in table 6.

Table 6: Numerical and experimental results comparison.

	Numerical model 1st mode frequency [Hz]	Experimental test 1st mode frequency [Hz]	Relative error
Assembly	400.92	271.44	47.70%
Interface structure	947.42	978.82	3.21%

The assembly's relative error is almost 50% which shows that there was some error in the numerical model. Since the interface structure results had a meaningless error (smaller than 10%) which confirms the model and the material approach developed before, a direct conclusion is that the problem was in the stiffness of the hardware system part. This one was excessively stiff in the numerical model. By knowing this, a new FEM model (figure 12) was develop using exactly the same approach than the previous model but with two significant changes:

- The linkage tubes were modelled as CBAR elements to take into account the tubes stiffness;
- The hardware structure is modelled as a 3D part with Tetra elements instead of the CONM2 mass element. This is done to take into account its inertia.

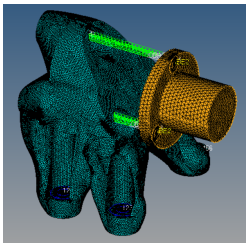

Figure 12: Modified FEM model.

The new comparison between the numerical and experimental results for the assembly can be seen in table 7. It is possible to see that this implementation was a success since the error is meaningless. The small errors in the assembly and structures results were probably caused by some error during the manufacturing or by the glue's stiffness contribution in the tubes' assembly (carbon tubes + glue + aluminum inserts). However, the author thinks that this simplified model (without the glue) was suitable for the application. Besides, the errors can also be caused by the lack of precision during the bolts tightening since an Allen's wrench was used instead of a torque wrench.

Table 7: Numerical and experimental results comparison after correction.

	Numerical model 1st mode frequency [Hz]	Experimental test 1st mode frequency [Hz]	Relative error
Assembly	282.73	271.44	4.16%

A simple sensitivity analysis was develop in order to increase the knowledge about the numerical approximations influence over the results in this problem. This is achieved through an analysis over two more models with the same initial model characteristics but with one significant difference. The 4 used models and respective differences were:

- Model 1 - Initial model with CONM2 and RBE2 elements;
- Model 2 - Similar to initial model but with CBAR elements;
- Model 3 - Similar to initial model but with 3D hardware structure;
- Model 4 - Similar to initial model but with 3D hardware structure and CBAR elements.

As expected, figure 13 shows that model 1 is the stiffest one, model 2 is the one with less stiffness and

model 3 and 4 are intermediary ones. However, it is also possible to see that model 4 was stiffer than model 3 which induces higher influence from the CBAR elements over the model results than the 3D hardware structure. Besides, the 3D hardware system inertia influence is dependent from the tubes stiffness as shown by the significant decrease in the frequency value of model 2 when compared to model 3 and 4. This makes sense due to the increase in the hardware structure's displacement. It is important to mention that even knowing that the CBAR have more influence, both changes have a significant influence in the model's accuracy.

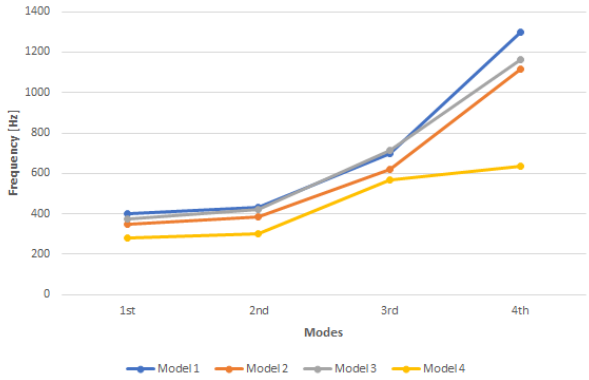

Figure 13: Sensivity analysis.

In order to correct and validate the numerical model, the experimental activity allowed a correlation between this one and the real one. Due to the correction made to the numerical model, this one complies with the reality which made this activity a success. The optimization approach and design were validated for this type of problem.

This activity was also a success due to the produced knowledge and sensitivity to this type of problems.

4. Final metal structure

With the optimization approach validated, the metal structure design feasibility assesment could be developed. The first step was to choose a suitable AM process and a material. A qualitative assessment was develop for the processes where the Powder Bed Fusion (PBF) methods were decided as the most suitable ones. Then, a market research was developed for the available materials within that processes where the several materials were compared through two ratios of interest: Young's modulus/Density and Yield strength/Density. The final choice was AlSi10Mg produced with SLM technique from Concept Laser [5] since based in the polymer experience, the stiffness will have more influence over the design and AlSi10Mg was the one with the highest Young's modulus/Density ratio.

4.1. Final metal structure design

An optimization cycle with two phases was developed in the same way as the optimization cycle used in the polymer. However, the material's properties were adapted as well as the 60G of magnitude for the inertial acceleration load cases. The optimization parameters are resumed in table 8.

Table 8: Optimization model parameters final structure.

E_0	75.00 GPa
x_{min}	0.001 Kg/m^3
p	3
ν	0.33
Conv. Val	<0.005
Dimension constraint	$\geq$ 0.5 mm
Frequency constraint	>2500 Hz

Both phases had different objectives and relevant findings that are enumerated next:

- **Phase 1:**
  - The design space is similar to the one used in the second phase of the polymer cycle in order to assess the necessity of the two front bolts;
  - From the obtained results, it was possible to conclude that the two front bolts are necessary since they have a significant continuity in the material to the rest of the structure. Besides, it was also possible to see some lack of design space freedom. This will be corrected in the next phase. As expected, the topology is similar to the one obtained during the polymer optimization.
- **Phase 2:**
  - The design space suffered big changes in this phase due to the necessity to use a torque wrench in the metal design. The design space was expanded to its maximum outside dimensions as in phase one of the polymer's cycle although a significant amount of it had been required by the torque wrench as can be seen in figure 14;
  - The obtained design does not fulfill the frequency constraint for the assembly since the optimization converged to a infeasible design. However, the frequency constraint imposed by the company is for the interface structure and not for the assembly. So, knowing that the interface structure alone will have a higher first

mode frequency as observed in the polymer's structure, the obtained concept design was accepted and the obtained model is fully operational as shown in figure 15.

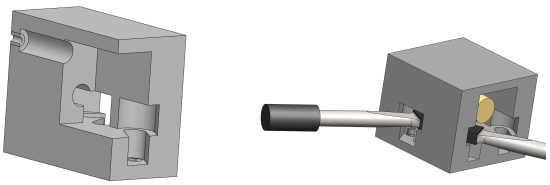

(a) Design space section cut. (b) Necessary space for torque wrench.

Figure 14: Design space for the final structure - phase 2.

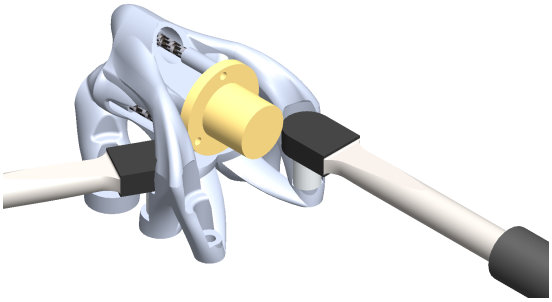

Figure 15: Fully operational assembly.

4.2. Final metal structure analysis

To verify that the final metal structure satisfies the initial requirements, an analysis was performed to assess its current performance. The numerical model was developed exactly in the same way as the modified FEM model for the polymer's structure.

The analysis results are depicted in table 9. It is possible to see that the assembly's first mode frequency is 457.86Hz which does not satisfy the optimization constraint, as expected. The final structure first mode frequency is 2521.19Hz which satisfies the initial requirement of a minimum of 2500Hz. The stress was not taken into account during the optimization process but in this analysis, its maximum value was 20.31MPa which is not significant for fatigue issues. This is supported by Uzan et al. [14], since their results on figure 7 showed that the minimum value that was found as fatigue stress limit for this material was higher than 50MPa.

Table 9: Optimized final metal structure design - analysis results.

	1st mode frequency [Hz]
Assembly	457.86
Final structure	2521.19

4.3. Final metal structure conclusions

The final structure optimization and design process were implemented with success since the structure fulfills the company's demands in terms of the first mode frequency. Besides, it is proved by figure 16 that the final structure does not influence the hardware system dynamic response, as supposed.

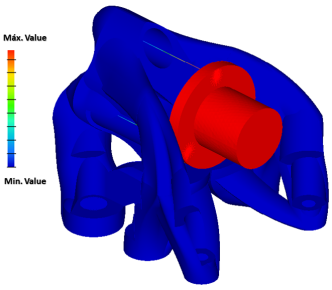

Figure 16: Final metal structure influence over hardware system's dynamic response.

It is also of extreme importance to compare the L-shape structure (company's current solution) to this optimized model as shown in table 10. Based in the results, it is possible to see that the first mode frequency of the final metal structure is 4.05% higher than the L-shape's one while the correspondent assembly's improvement is 9.14%. In terms of mass, a significant reduction of 75.72% was achieved. This makes the final metal structure stiffer, significantly lighter and capable of increasing the first mode frequency with the hardware system mounted.

5. Conclusions

Along this work development, several objectives were achieved. The benchmark examples brought new knowledge and sensibility to TO problems as well as the opportunity to decide which of both commercial softwares is more suitable to this application.

With this knowledge, an optimization cycle process was developed with several load cases and several optimization steps which had important conclusions that converged to a lighter and operational design. A 3D printed polymer was used instead of a metal in order to produce a prototype and test it. The polymer was subjected to mechanical characterization tests that proved its isotropic behaviour in the elastic regime and the correspondent properties of interest. The 3D printed optimized part was produced, treated in post-processing and tested in *Active Space Technologies'* shaker with success. The test results were correlated with the numerical model and after some corrections, the model was validated since an error of 4.16% and 3.21% were achieved for the assembly and interface structure, respectively. This experimental activity validated the TO methodology implemented.

Table 10: Final structure and L-shape comparison.

	L-shape	Final metal structure	Improvement	L-shape assembly	Final metal structure assembly	Improvement
Mass [g]	2175.81	528.21	-75.72%	-	-	-
1st mode frequency [Hz]	2423.14	2521.19	4.05%	419.51	457.86	9.14%

The final metal interface structure was developed using the validated TO methodology where a significant improvement was achieved when this structure is compared to the company's L-shape current solution. An increment of 4.05% in the first mode frequency and a reduction of 75.72% in the mass makes this structure a better solution. The final metal structure complies with all the company's demands being important to refer its non-influence over the hardware system dynamic response and the increase of the assembly's first mode frequency when compared to the L-shape's one (increment of 9.14%).

This design success proved the advantageous relation between topological optimization and additive manufacturing due to its complex geometry. From now on, the develop methodology can also be used to design support structures for flight hardware.

5.1. Future Work

This work established an optimization and design process on which some future relevant improvements may be applied, such as:

- Characterization of the metal material and its optimized structure testing even though the optimization methodology is already validated.
- Taking into account the AM procedures for the metals during the design. Problems as the support material removal during the post-processing can happen and in this design, they probably need to be there to prevent warping and distortion during the manufacturing;
- The usage of lattice structures to simulate an element density. Lattice structures are known by their high stiffness and strength to low mass values [12]. 3D printing machines already have a very refined accuracy that enables the production of lattice structures precisely. So, the lattice structures shall be used to simulate an element density in order to use topology optimization true optimum and not only as a conceptual design.

References

[1] 3D SYSTEMS. VisiJet M3 Crystal (MJP), April 2018.

[2] Altair Engineering. *Practical Aspects of Finite Element Simulation: A Study Guide*. 3^{rd} edition, May 2015.

[3] M. P. Bendse and O. Sigmund. *Topology Optimization: Theory, Methods and Applications*. Springer, 2003. ISBN: 3-540-42992-i.

[4] Brüel and Kjaer. Accelerometers and charge amplifiers, 2017.

[5] CONCEPTLASER. Materials, February 2018.

[6] J. N. Reddy. *An Introduction to the Finite Element Method*. McGraw-Hill Primis, 3^{rd} edition, 2006.

[7] K. Liu and A. Tovar. An efficient 3d topology optimization code written in matlab. *Structural and Multidisciplinary Optimization*, 50:1175–1196, December 2014.

[8] MSC Software. *MSC Nastran 2017.1 Documentation*. 2017.

[9] A. Remouchamps, M. Bruyneel, C. F. S., and G. S. Application of a bi-level scheme including topology optimization to the design of an aircraft pylon. *Struct Multidiscip Optim*, 44:739–750, 2011.

[10] G. I. N. Rozvany. Aims, scope, methods, history and unified terminology of computer-aided topology optimization in structural mechanics. *Structural and Multidisciplinary Optimization*, 21(2):90–108, April 2001.

[11] O. Sigmund. A 99 line topology optimization code written in matlab. *Structural and Multidisciplinary Optimization*, 21:120–127, April 2001.

[12] N. S. Sripada. *A Methodology for Topology and Lattice Stucture Optimization of a cargo drone motor mount*. Master's thesis, Mechanical Engineering, The University of Texas at Arlington, December 2017.

[13] M. Tomlin and J. Meyer. *Topology Optimization of an Additive Layer Manufactured (ALM) Aerospace Part*. EADS Innovation Works, 2011.

[14] N. E. Uzan, R. Shneck, O. Yeheskel, and N. Frage. Fatigue of alsi10mg specimens fabricated by additive manufacturing selective laser melting (am-slm). *Materials Science and Engineering: A*, 704:229237, September 2017.